

Semi-Persistent Scheduling in NR Sidelink Mode 2: MAC Packet Reception Ratio Model and ns-3 Validation

Liu Cao, *Student Member, IEEE*, Sumit Roy, *Fellow, IEEE*, Collin Brady, *Student Member, IEEE*

Abstract—5G New Radio (NR) Sidelink (SL) has demonstrated the promising capability for infrastructure-less cellular coverage. Understanding the fundamentals of the NR SL channel access mechanism, Semi-Persistent Scheduling (SPS), which is specified by the 3rd Generation Partnership Project (3GPP), is a necessity to enhance the NR SL Packet Reception Ratio (PRR). However, most existing works fail to account for the new SPS features introduced in NR SL, which might be out-of-date for comprehensively describing the NR SL PRR. The existing models ignore the relationships between SPS parameters and, therefore, do not provide sufficient insights into the PRR of SPS. This work proposes a novel SPS PRR model incorporating MAC collisions based on new features in NR SL. We extend our model by loosening several simplifying assumptions made in our initial modeling. The extended models illustrate how the PRR is affected by various SPS parameters. The computed results are validated via simulations using the network simulator (ns-3), which provides important guidelines for future NR SL enhancement work.

Index Terms—NR SL, Mode 2, SPS, MAC, Performance analysis, Validation.

I. INTRODUCTION

SIDELINK (SL) is a 3rd Generation Partnership Project (3GPP) standardized technology that enables direct user-to-user communications, without the assistance of traditional cellular networks [1]. Current SL (Release 16) has evolved from the Proximity Services (ProSe) protocol, defined in Release 12 to support public safety applications, [2]. As of Release 16, SL operates in modes 1 and 2, supporting direct communication among multiple User Equipment (UEs). The key difference: in mode 1, the resources used by the UE-to-UE link are allocated by the base station (gNB), whereas in mode 2, resources are selected autonomously without any gNB coordination.

A promising application for SL is support for mission-critical data connectivity needs with Ultra-Reliable Low-Latency Communications (URLLC) requirements. These characteristics are helpful in various scenarios, such as Vehicle-to-Everything (V2X), various first-responder use, and industrial IoT, leading to continued interest in expanding SL scope. SL mode 2 supports the

formation of local-area, ad-hoc networks without cellular infrastructure (e.g., remote areas or complex propagation environments such as underground, undersea, or airborne). All such applications also bring new technical challenges for network formation over SL, e.g., the necessity to re-architect key primitives such as neighbor discovery, authentication, and efficient channel acquisition [1]. Because of this, enhancements to the current SL continue to be an active topic in 3GPP Rel-18/Rel-19 with several study items [3].

This work focuses on performance evaluation of the NR SL mode 2 Semi Persistent Scheduling (SPS) protocol, a distributed media access control (MAC) scheme that was initially introduced in Long Term Evolution (LTE) SL mode 4 (Release 14) and subsequently adopted for 5G NR. SPS includes a *distributed sensing* feature that enables all UEs in a decentralized network to *monitor the share channel and determine which resources are in use, and avoid utilizing these (in-use resources) for upcoming message transmissions*. SL design has evolved from the original Rel-14 specifications to include 5G NR numerology, operate over multiple frequency bands such as FR2 (mmWave), and support more communication types (unicast and groupcast in addition to broadcast); correspondingly, this has led to updates in SPS design in terms of new parametrization to meet the reliability requirements faced with network reconfiguration and scalability.

In this work, we focus on analyzing broadcast NR SL mode 2 that uses SPS for basic safety/status messaging in C-V2X scenarios. A significant set of prior work analyzing SPS performance has been primarily based on simulations [4]–[11]. For instance, [5]–[7] proposed different simulation frameworks to study LTE/NR V2X. While a custom framework was developed in Matlab in [5], [6] and [7] built modules in Objective Modular Network Testbed in C++ (OMNeT++) and network Simulator 3 (ns-3), respectively. Both [8] and [9] used the simulation framework from [5] to explore the effects of varying the numerology and the physical (PHY)/MAC parameters on the Packet Reception Ratio (PRR) in V2X, respectively. In summary, none of these studies undertake any analytical modeling of SPS performance. A few efforts have been devoted to SL MAC and PHY analysis in recent years [12]–[16], exploring the impact of system parameters and network conditions on SL performance. For example, [12], [13] focused on the cross-layer (MAC + PHY) modeling of the C-V2X SPS in a vehicle platooning scenario. A novel discrete-time Markov chain (DTMC) approach was presented in [17] to calculate the average delay, collision probability and channel utilization in LTE

This work was presented in part at the Workshop on ns-3 (WNS3) 2023: <https://www.nsnam.org/tutorials/consortium23/NR-C-V2X-Tutorial-WNS3-2023.pdf>.

Liu Cao, Sumit Roy, and Collin Brady are with the Department of Electrical and Computer Engineering, University of Washington, Seattle, WA, USA (e-mail: {liuca, roy, collinb}@uw.edu).

TABLE I: Glossary

Notation	Definition
T_{RRI}	Duration of Resource Reservation Interval (RRI), millisecond
$R_{c,init}(T)$	Initial reselection counter at time T
$R_c(T)$	Reselection counter at time T
p_k	Resource keeping probability
T_g	The time the reference UE generates a packet
N_{sc}	Number of subchannels
t_s	Slot duration, millisecond
N_r	Total number of PRBs in each RRI
R_c^{UE0}	UE 0's reselection counter
$R_{c,init}^{UE0}$	UE 0's initial reselection counter
P_{COL}	Total MAC collision probability
$P_{COL,1}$	The probability for Collision Event 1
$P_{COL,2}$	The probability for Collision Event 2
π_i	Probability that $R_c = i$
N_{UE}	Total number of UEs
$P_s(n)$	The probability that n UEs reselect within UE 0's selection window
N_a	Number of available (unoccupied) PRBs in the selection window
N_o	Number of occupied PRBs in the selection window
N_c	Number of packets in an occupied PRB where collisions happen
$P_r(n)$	The probability of n -fold collision given that n UEs reselect
$P_{COL,2}^{E1}$	$P_{COL,2}$ due to E1
$E1$	Collision during $[T_1, T_1 + T_{RRI}]$, and $R_{c,init}^{UE0} = R_c^{UE1}$ at $T = T_1 + T_{RRI}$
$P_{COL,2}^{E2}$	$P_{COL,2}$ due to E2
$E2$	Collision during $[T_1, T_1 + T_{RRI}]$, and $R_{c,init}^{UE0} < R_c^{UE1}$ at $T = T_1 + T_{RRI}$
$P_{COL,2}^{E3}$	$P_{COL,2}$ due to E3
$E3$	Collision during $[T_1, T_1 + T_{RRI}]$, and $R_{c,init}^{UE0} > R_c^{UE1}$ at $T = T_1 + T_{RRI}$
P_{HD}	Probability that Half-duplex effects happen
PRR	Packet reception ratio
N_{Se}	Number of packets that each UE sends per RRI
X	Minimum proportion requirement of available PRBs
$d_{t,r}$	Transmission range

SL mode 4. However, the proposed Markov-based SPS analysis incorporated only limited SPS parameters - the reselection counter and the selection window size. The authors in [14], [15] modeled the PRR and the access collision probability for LTE SL mode 4, respectively. However, they only focused on the legacy SPS protocol for LTE SL and failed to account for the new NR SL SPS features, such as the multiple packet transmission that significantly impacts the PRR. Meanwhile, most existing analytical models for the legacy SPS protocol may not provide insights into how SPS parameters relate to each other for determining the SL performance, such as PRR. However, understanding their mutual impacts is important for the performance enhancement of future beyond 5G (B5G) and 6G SL applications.

The primary contribution of this work is the *first* complete analytical model for C-V2X mode 2 MAC collision events, which is used to derive the PRR. Our model accounts for all key MAC parameters present in V2X mode 2, including the resource-keeping probability, the number of duplicate transmissions, and the proportion of available PRBs for reselection. We investigate the effects of these MAC parameters on PRR and on a set of intermediate performance metrics such as the Layer-2 packet collision probability or the number of available resources. Finally, we provide results based on ns-3 based V2X simulation that corroborates our analysis and provides independent simulation validation.

The rest of this paper is organized as follows. Sec. II describes the system setup and defines the MAC collision events. Sec. III provides the analytical model for the defined collision events and PRR for some MAC parameters, while Sec. IV updates the model of collision probabilities and PRR to incorporate the number of duplicate transmissions. Sec. V then describes and shows results

from the simulation regime used to validate the model.

II. SYSTEM SETUP

Consider a typical SL mode 2 scenario where static UEs are randomly distributed in a local region such that the resulting network is fully connected. SL packet traffic sent from each UE is periodic, representing the Basic Safety Message (BSM) class, and uses the sensing-based Semi-Persistent Scheduling (SPS) defined in [3], [18] for channel access. An SL *resource pool*¹ comprised of a set of contiguous sub-channels² in the frequency domain and slots in the time domain, enables transmission of (data) Transport Block (TB) which, for our purposes, constitutes a single SL Layer-2 packet [19]. This combination of one sub-channel and one slot to transmit a TB is a Physical Resource Block (PRB) that constitutes the unit resource in sensing-based SPS. We assume a perfect PHY-layer as befits a pure MAC analysis, i.e., any Layer-2 packet sent from a source is received perfectly by all intended receivers if not interfered with due to simultaneous transmission(s) by other UE sources.

A. Sensing-based SPS: Recap

Sensing-based SPS [20], [21] is a distributed MAC protocol for NR SL that seeks to achieve collision avoidance based on predictive resource reservation by UEs over a resource reservation interval (RRI), T_{RRI} . A flowchart of the SPS procedure is shown in Fig. 1, which can be decomposed into two stages for purposes of understanding key aspects of protocol operation.

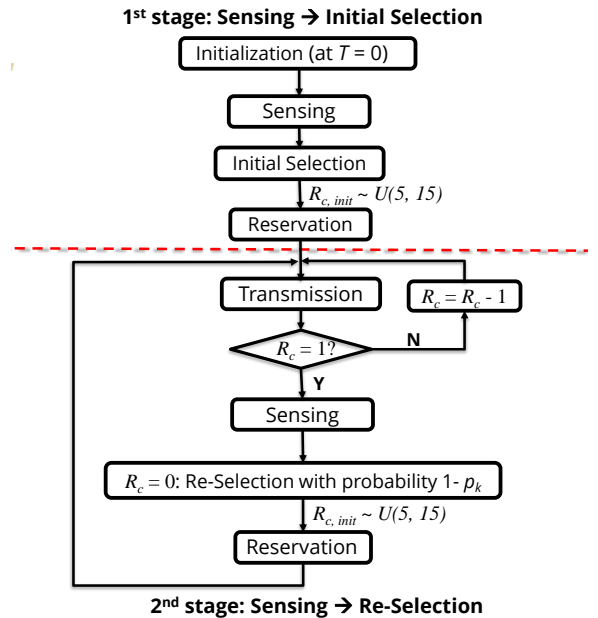


Fig. 1: SPS MAC Procedure.

¹A set of available time/frequency resources dedicated for SL TB transmissions.

²A subchannel is composed of a network maintainer configured number of resource blocks, which are in turn composed of 12 subcarriers whose bandwidth is defined by the subcarrier spacing.

Stage 1: Sensing \rightarrow Initial Selection. This is the initial stage where a reference UE performs sensing-based initial selection for subsequent resource reservation. A reference UE first determines the PRBs occupied by other UEs during the sensing window³ via comparison to a reference signal received power (RSRP) threshold and then excludes those occupied PRBs for the subsequent reservation during selection window. The reference UE then **randomly** selects one among the remaining available PRBs in the selection window (for transmission of Layer-2 packet) and simultaneously chooses a *Reselection counter* $R_{c,init}$, implying reservation of the initially selected PRB for subsequent $R_{c,init}$ transmissions. $R_{c,init}$ is selected as independent and identically distributed (i.i.d.) random variable from the uniform distribution $U(5, 15)$ ⁴. The counter is decremented by 1 after each T_{RRI} . An example is illustrated in Fig. 2.

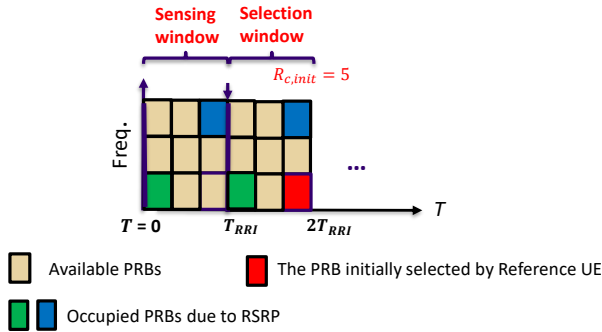


Fig. 2: SPS Stage 1: Reference UE Case.

Stage 2: Sensing \rightarrow Reselection. In this stage, the reference UE starts packet transmissions, counts down the reselection counter until $R_c = 0$ and then enters reselection of PRBs:

- *Exclusion of occupied PRBs during the sensing window.* Since SL UEs are typically half-duplex (i.e., incapable of transmitting and receiving simultaneously), the reference UE cannot detect the RSRP of PRBs in the same slot when it transmits. Thus, in the sensing window for reselection, reference UE will exclude all ‘occupied’ PRBs due to not only exceeding the RSRP threshold but also the half-duplex constraint.
- *Reselection.* When the reference UE’s $R_c = 0$, it randomly **re-selects** one of the available PRBs with probability $1 - p_k$ during the selection window while persisting with the prior reserved PRB selection with probability p_k . $p_k \in [0, 0.8]$ is the *resource keeping* parameter specified in 3GPP standard and is identical for all UEs in the network. Such a reselection cycle is repeated in Stage 2 and is illustrated via example in Fig. 3. Since UE performs the process of sensing and initial

selection only once during the 1st stage while repeating the process of sensing and reselection during the 2nd stage, the packet reception ratio (PRR) in the long term (i.e., the steady state) is determined by the 2nd stage. We thereby develop the PRR model based on the events in the 2nd stage.

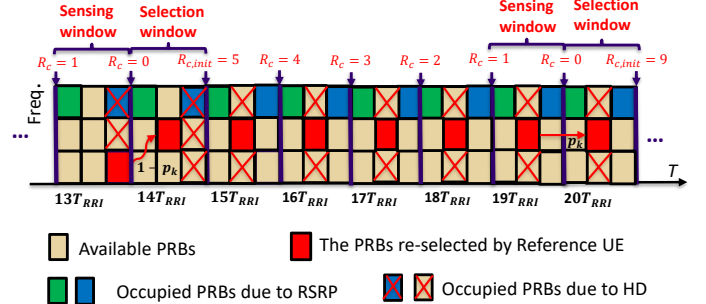


Fig. 3: SPS Stage 2: Reference UE Case.

The structure of the Sensing and Selection windows is shown in Fig. 4. Each UE reserves a PRB for a periodic packet transmission within T_{RRI} . For simplicity, the *Sensing window* covers the duration $[T_g - T_{RRI}, T_g]$ ⁵, where T_g is the packet generation instant at $R_c = 0$, followed by the *Selection window* over the duration $[T_g, T_g + T_{RRI}]$ ⁶. If we denote the slot duration as t_s that depends on the numerology, the total number of slots within the sensing/selection window equals T_{RRI}/t_s and consequently, the total number of PRBs within the sensing/selection window is given by

$$N_r = \frac{T_{RRI} N_{sc}}{t_s}. \quad (1)$$

It should be noted the selection window size can range from 1 slot upto T_{RRI} according to the 3GPP standard. N_r can be readily adapted by replacing T_{RRI} in Eq. (1) with any selection window size from 1 slot to T_{RRI} . In this paper, however, we consider the selection window size to be T_{RRI} , which more adequately characterizes the collision events and key SPS parameters with their mutual impacts on the PRR model.

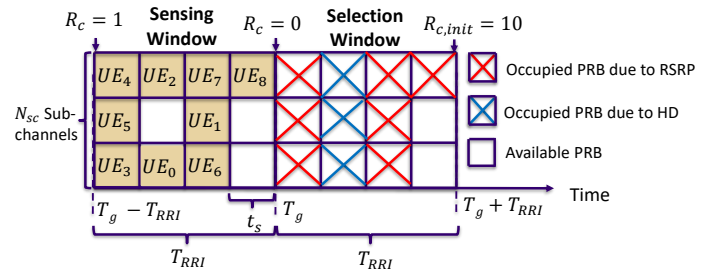


Fig. 4: Sensing Window and Selection Window.

³The sensing window covers one or multiple T_{RRI} defined in the 3GPP standard, depending on the upper layer setup.

⁴ $R_{c,init}$ range varies if $T_{RRI} < 100$ ms but always satisfies $R_{c,init} \in U(5, 15)$ for $T_{RRI} \geq 100$ ms per the 3GPP standard. Since T_{RRI} is defined at the application layer, it is not the variable of interest for the MAC-layer analysis. For simplicity, we consider the SL applications with $T_{RRI} \geq 100$ ms, thus $R_{c,init} \in U(5, 15)$ range always holds.

⁵Per the 3GPP standard, the sensing Window is defined as the duration $[T_g - T_{RRI}, T_g - T_0]$, where the processing time T_0 duration is typically equal to 1 or 2 slots, which is significantly smaller than T_{RRI} duration.

⁶In such a selection window, the access delay (the elapsed time from the instant packet generates to the instant it transmits) ranges from 1 slot to the maximum packet delay budget, i.e., T_{RRI} .

B. MAC Collision Events in the Selection Window

MAC collision happens when two (or more) UEs transmit in the same PRB, and all other UEs fail to decode any transmitted packets. Such a MAC collision event starts in a selection window and is followed by consecutive collisions at the next several RRI. When reference UE 0's R_c decrements to 0, it enters the selection window and either performs reselection with probability $1 - p_k$, or does not with probability p_k . The MAC collisions in the selection window are thereby conditioned on whether UE 0 performs (or does not perform) reselection in the selection window, i.e.:

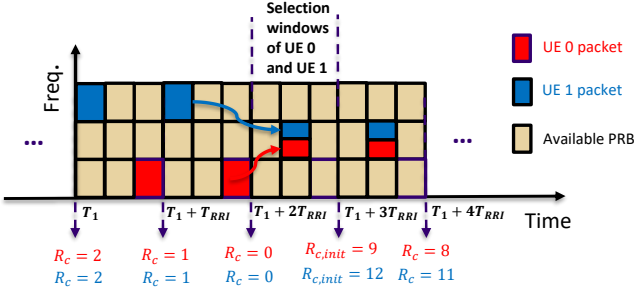
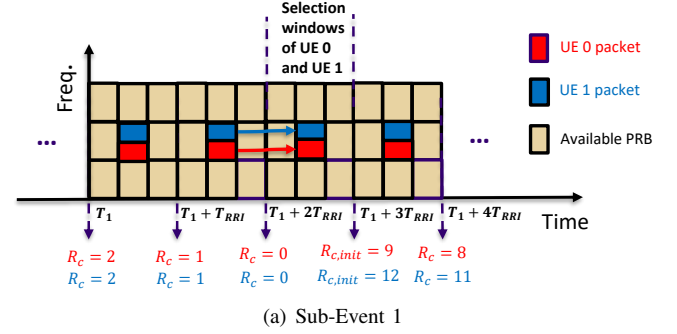


Fig. 5: Collision Event 1.

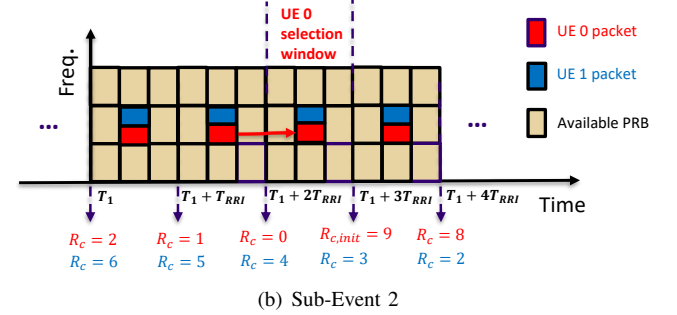
Collision Event 1 - UE 0 performs reselection in the selection window and collides with another UE that also performs reselection. In Fig. 5 we see when UE 0's R_c decrements to 0 at $T = T_1 + 2T_{RRI}$, UE 1's R_c also decrements to 0, indicating that both enter the selection window simultaneously. Each performs reselection by randomly and independently choosing one of 7 available PRBs out of $N_r = 9$ PRBs in the selection window during $[T_1 + 2T_{RRI}, T_1 + 3T_{RRI}]$. If two UEs select the same PRB, it leads to MAC collision in their overlapping selection window. At $T = T_1 + 3T_{RRI}$, $R_c^{UE0}(T) = 9$ while $R_c^{UE1}(T) = 12$, indicating that the PRB reselected by UE 0 and UE 1 in the selection window will be reserved for the following 9 RRIs and 12 RRIs, respectively. The number of consecutive collisions is thus $\min\{R_c^{UE0}(T), R_c^{UE1}(T)\}$. Since both $R_c^{UE0}(T)$ and $R_c^{UE1}(T) \in [5, 15]$, the number of consecutive collisions right after UE 0's selection window lies in the range [5, 15].

Collision Event 2 - UE 0 does not perform reselection in the selection window and continues to collide with a UE that it has previously collided with in prior RRIs. Collision Event 2 includes two collision sub-events that depend on the collided UE's R_c state at the moment UE 0's $R_c = 0$:

- **Sub-event 1 - Collided UE's $R_c = 0$ when UE 0's $R_c = 0$.** In Fig. 6(a) we see UE 0's R_c decrements to 0 at $T = T_1 + 2T_{RRI}$, meanwhile the collided UE 1 also decrements to 0. Then, both UEs do not perform reselection, indicating that both persist with the PRB reserved in the prior selection window to the current, i.e., over $[T_1 + 2T_{RRI}, T_1 + 3T_{RRI}]$. Since both UEs have collided with each other by reserving the same PRB in the prior RRIs, MAC collisions between UE 0 and UE 1 will continue in their overlapping selection window. The number of consecutive collisions right after UE 0's selection window under Collision Event 2 Sub-event 1



(a) Sub-Event 1



(b) Sub-Event 2

Fig. 6: Collision Event 2.

is still $\min\{R_c^{UE0}(T), R_c^{UE1}(T)\}$ which lies in the range [5, 15].

- **Sub-event 2 - Collided UE's $R_c \neq 0$ when UE 0's $R_c = 0$.** In Fig. 6(b) we see UE 0's R_c decrements to 0 at $T = T_1 + 2T_{RRI}$, meanwhile the collided UE 1's $R_c = 4$. In the UE 0's selection window during $[T_1 + 2T_{RRI}, T_1 + 3T_{RRI}]$, UE 0 does not perform reselection by sticking with the PRB reserved in the prior RRIs; meanwhile, UE 1 still uses the PRB reserved in the past RRIs to send packet because UE 1's R_c has not decremented to 0 yet. Since both UEs have collided with each other by reserving the same PRB in the RRIs prior to UE 0's selection window, MAC collisions will continue between UE 0 and UE 1 after UE 0's selection window. The number of consecutive collisions after UE 0's selection window under Collision Event 2 Sub-event 2 is $\min\{R_c^{UE0}(T), R_c^{UE1}(T)\}$. As $R_c^{UE0}(T) \in [5, 15]$ and $R_c^{UE1}(T) \in [0, 14]$, the number of consecutive collisions after UE 0's selection window under Collision Event 2 Sub-event 2 lies in the range [0, 14].

Finally, note that if UE 0 does not suffer a collision in its selection window, no further collisions occur in the following R_c^{UE0} RRIs after UE 0's selection window. Since the PRB selected by UE 0 in the selection window is reserved for the following R_c^{UE0} RRIs, this occupied PRB must be excluded in the following R_c^{UE0} RRIs for any UE that enters its selection window in this interval.

III. SPS PRR ANALYTICAL MODEL

As Sec. II shows, the collision of reference UE 0 in the selection window includes Collision Events 1 and 2. Let P_{COL} be

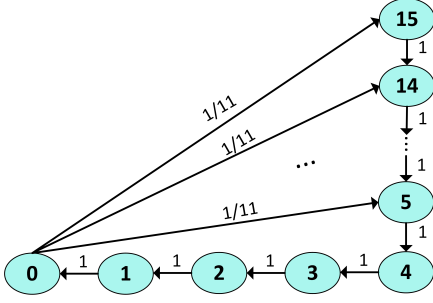


Fig. 7: Reselection Counter (R_c) State Diagram.

the total probability of MAC collision, $P_{COL,1}$ as the probability for Collision Event 1, and $P_{COL,2}$ as the probability for Collision Event 2. Since Events 1 and 2 are mutually exclusive,

$$P_{COL} = P_{COL,1} + P_{COL,2}, \quad (2)$$

where $P_{COL,1}$ and $P_{COL,2}$ are analyzed in the following sections.

A. Performance Analysis - Reselection Counter State

Fig. 7 shows R_c state diagram for our SPS model, identical for all UEs. At any nT_{RRI} , the corresponding $R_c(nT_{RRI}) \in [0, 15]$. If $R_c(nT_{RRI}) = 0$, it is randomly re-initialized s.t. $R_{c,init}((n+1)T_{RRI}) \in [5, 15]$. Thus, the probability that

$$\Pr\{R_{c,init}((n+1)T_{RRI}) = i | R_c(nT_{RRI}) = 0\} = \frac{1}{11}. \quad (3)$$

Denote π_i as the probability that $R_c(nT_{RRI}) = i, 0 \leq i \leq 15$. According to Fig. 7, π_i satisfies

$$\pi_i = \begin{cases} \pi_0 & \text{for } 0 \leq i \leq 4, \\ \frac{1}{11}\pi_0 + \pi_{i+1} & \text{for } 5 \leq i \leq 14, \\ \frac{1}{11}\pi_0 & \text{for } i = 15. \end{cases} \quad (4)$$

Using the normalization condition $\sum_{i=0}^{15} \pi_i = 1$, and solving (4), we obtain $\pi_0 = \frac{1}{11}$. Notice that the proposed R_c state diagram in Fig. 7 can be easily extended to cover different $R_{c,init}$ ranges for $T_{RRI} < 100$ ms, if necessary, which leads to a moderate revision in Eq. (4) following a similar calculation manner. Since investigating the impact of the $R_{c,init}$ range is not the focus in this paper, using $R_{c,init} \in [5, 15]$ for $T_{RRI} \geq 100$ ms is used for model simplicity.

We consider asynchronous R_c decrement whereby UEs' R_c counters follow independent clocks. Therefore, UEs' selection windows will partially overlap (when their R_c decrement to 0) within an T_{RRI} . Fig. 8 shows a two-UE example for asynchronous R_c decrement, where UE 0's selection window spans two consecutive RRIs of UE 1, either of which may be UE 1's selection window. Note that since the probability that any UE 1 RRI is its selection window equals π_0 , the probability that UE 0's selection window partially overlaps with UE 1's is $2\pi_0$.

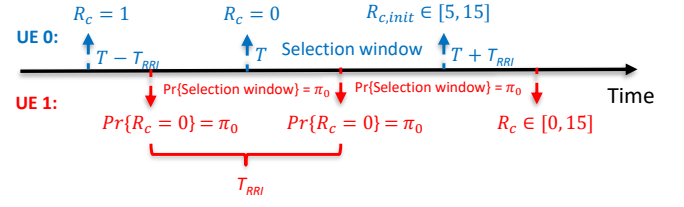


Fig. 8: Asynchronous R_c Decrement.

B. Performance Analysis - Collision Event 1

Collision Event 1 happens if at least one of the other UEs also selects the same available PRB as UE 0 (reference UE). Thus, Collision Event 1 is triggered by the reselection behavior of multiple UEs in the overlapping selection window. Suppose UE 0's $R_c = 0$ at time T and UE 0 then performs reselection in its selection window during $[T, T + T_{RRI}]$. If another UE among N_{UE} UEs participates in reselection during $[T - T_{RRI}, T + T_{RRI}]$, its R_c should first decrement to 0 during $[T - T_{RRI}, T + T_{RRI}]$ (whose probability is $2\pi_0$), and then this UE performs reselection with probability $1 - p_k$. As each UE's R_c state is independent, if any n out of total N_{UE} UEs participate in reselection during $[T - T_{RRI}, T + T_{RRI}]$, the corresponding probability follows the binomial distribution, given by

$$\Pr\{n \text{ UEs } R_c = 0, \text{ Reselection} | R_c^{UE0} = 0, \text{ Reselection}\} = P_s(n) = \binom{N_{UE}}{n} (2\pi_0(1 - p_k))^n (1 - 2\pi_0(1 - p_k))^{N_{UE} - n}. \quad (5)$$

The UE 0 and n UEs then randomly reselect one of the available (unoccupied) PRBs in the overlapping selection window. The collision occurs if at least one of these n UEs selects the same available (unoccupied) PRB as UE 0. We define such a collision due to n -UE participating in reselection in the overlapping selection window as **n -fold collision**. Note that the number of available PRBs in the selection window N_a depends on the total number of PRBs in the selection window N_r and the number of occupied PRBs in the selection window N_o , i.e.,

$$N_a = N_r - N_o, \quad (6)$$

where both N_a and N_o are random variables. Since each UE with a packet to send needs to select a PRB in each RRI (including the selection window), N_{UE} UEs will occupy N_{UE} PRBs in each RRI if no collision happens (i.e., $N_o = N_{UE}$, a fixed number). However, in the event of collisions, $N_o < N_{UE}$ is a random variable. The average number of occupied PRBs \bar{N}_o in the selection window can be expressed in terms of the total MAC collision probability,

$$\bar{N}_o = N_{UE} - P_{COL}N_{UE} + \frac{P_{COL}N_{UE}}{\bar{N}_c}, \quad (7)$$

where P_{COL} is the total MAC collision probability (Collision Event 1 + Collision Event 2) to be determined, and the random variable $\bar{N}_c \geq 2$ is the number of UEs in an occupied PRB where the collision happens. In Eq. (7), $P_{COL}N_{UE}$ represents the average number of UEs who collide with other UEs in the selection window. Thus $\frac{P_{COL}N_{UE}}{\bar{N}_c}$ represents the average number

of occupied PRBs where collisions happen in the selection window, while $N_{UE} - P_{COL}N_{UE}$ represents the average number of occupied PRBs where collisions do not happen in the selection window. As Eq. (7) suggests, \bar{N}_o will decrease if \bar{N}_c increases. Then the average number of available (unoccupied) PRBs in the selection window, \bar{N}_a , is given by

$$\bar{N}_a = N_r - \bar{N}_o = N_r - N_{UE} + \frac{(\bar{N}_c - 1)P_{COL}N_{UE}}{\bar{N}_c}. \quad (8)$$

Given \bar{N}_a available (unoccupied) PRBs in the selection window, the probability that one of n UEs collides with UE 0 by reselecting the same available PRB is $1/\bar{N}_a$. As a result, the probability that n -fold collision happens (i.e., at least one of n UEs select the same PRB as UE 0) given that n UEs participate in reselection is

$$\begin{aligned} & \Pr\{n\text{-fold Collision} | n \text{ UEs } R_c = 0, \text{ Reselection}\} \\ &= P_r(n) = 1 - \left(1 - \frac{1}{\bar{N}_a}\right)^n. \end{aligned} \quad (9)$$

Therefore, the probability that n -fold collision happens given that UE 0 performs reselection in the selection window is $P_r(n)P_s(n)$. Considering all n ($1 \leq n \leq N_{UE}$), we can obtain the collision probability when UE 0 performs reselection in the selection window as:

$$\Pr\{\text{Collision} | R_c^{UE0} = 0, \text{ Reselection}\} = \sum_{n=1}^{N_{UE}} P_r(n)P_s(n). \quad (10)$$

Substituting Eq. (5) and (9) into Eq. (10), yields

$$\begin{aligned} & \Pr\{\text{Collision} | R_c^{UE0} = 0, \text{ Reselection}\} \\ &= 1 - \left(1 - \frac{2\pi_0(1-p_k)}{\bar{N}_a}\right)^{N_{UE}}. \end{aligned} \quad (11)$$

$P_{COL,1}$ is thus expressed as

$$\begin{aligned} P_{COL,1} &= \Pr\{\text{UE 0 Reselection} | R_c^{UE0} = 0\} \\ &\cdot \Pr\{\text{Collision} | R_c^{UE0} = 0, \text{ Reselection}\} \\ &= (1-p_k) \left[1 - \left(1 - \frac{2\pi_0(1-p_k)}{\bar{N}_a}\right)^{N_{UE}}\right], \end{aligned} \quad (12)$$

where \bar{N}_a is given by Eq. (8). Note that for $p_k = 0$, $P_{COL} = P_{COL,1}$ from Eq. (2) and hence $P_{COL,1}$ can be directly determined by solving Eq. (8) and (12) simultaneously. However for $p_k > 0$, $P_{COL,1}$ cannot be directly determined yet because $P_{COL,1}$ is a function of $P_{COL,2}$. Meanwhile, according to Eq. (12), $P_{COL,1}$ decreases as \bar{N}_a increases, and hence from Eq. (8), $P_{COL,1}$ will decrease as \bar{N}_c increases.

C. Performance Analysis - Collision Event 2

Collision Event 2 happens if UE 0 has collided with at least one of the other UEs in UE 0's most recent selection window, and collision will continue in UE 0's current selection window if both UE 0 and the collided UE(s) do not change the PRB after UE 0's most recent selection window. Similar to Collision Event

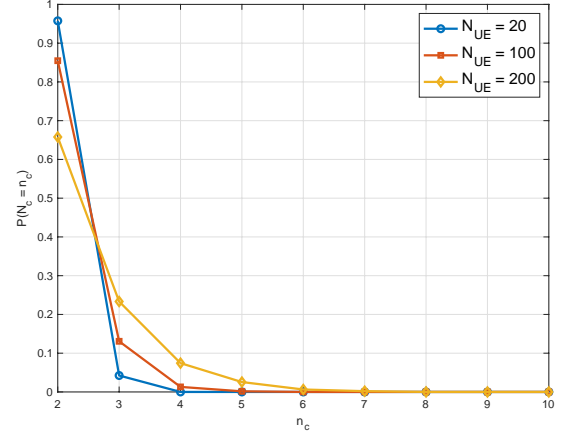


Fig. 9: The Proportion of n_c -Packet Collision at Different N_{UE} .

1 potentially involving multiple (> 2) packets/UEs as indicated by Eq. (9) resulting in n -fold collision, Collision Event 2 may also involve multiple packets/UEs. For instance, if $n = 10$, ten other UEs participate in reselection within the overlapping selection window as UE 0, the number of collided packets/UEs in a collision N_c can be up to 10. However, Fig. 9 shows that the 2-packet/UE collision (i.e., $N_c = 2$) probability dominates for all N_{UE} , as observed from data gathered through ns-3 simulations, especially in under-saturated condition. Since our analytical model is aimed at the under-saturated condition, we hereafter assume that only the 2-packet/UE collisions constitute Collision Event 2 to simplify the analytical model, as shown in Fig. 10.

Since Collision Event 2 occurs conditioned on the events in UE 0's most recent previous selection window during $[T_1, T_1 + T_{RR1}]$, as represented by the following event sets:

- $E1 = \left\{ \text{Collision during } [T_1, T_1 + T_{RR1}], \text{ and } R_{c,init}^{UE0} = R_c^{UE1} \text{ at } T = T_1 + T_{RR1} \right\}$, shown in Fig. 10(a). Then $R_c^{UE0} = R_c^{UE1} = 0$ at the beginning of UE 0's current selection window, and collision will continue into UE 0's current selection window if both UEs do not perform reselection (with probability = p_k^2). Since the probability that $E1$ happens is given by:

$$\Pr\{E1\} = P_{COL} \cdot \Pr\{R_{c,init}^{UE0} = R_c^{UE1}\}, \quad (13)$$

where $\Pr\{R_{c,init}^{UE0} = R_c^{UE1}\} = \Pr\{R_c^{UE1} = 0 | R_c^{UE0} = 0\} = 2\pi_0$. Then, the probability that Collision Event 2 happens due to $E1$ is thereby derived as

$$P_{COL,2}^{E1} = \Pr\{\text{Collision} | E1\} \cdot \Pr\{E1\}. \quad (14)$$

where $\Pr\{\text{Collision} | E1\} = p_k^2$.

- $E2 = \left\{ \text{Collision during } [T_1, T_1 + T_{RR1}], \text{ and } R_{c,init}^{UE0} < R_c^{UE1} \text{ at } T = T_1 + T_{RR1} \right\}$, shown in Fig. 10(b). Then $R_c^{UE0} = 0$ while $R_c^{UE1} > 0$ at the beginning of UE 0's current selection window, and collision will continue in the current reselection window if UE 0 does not perform

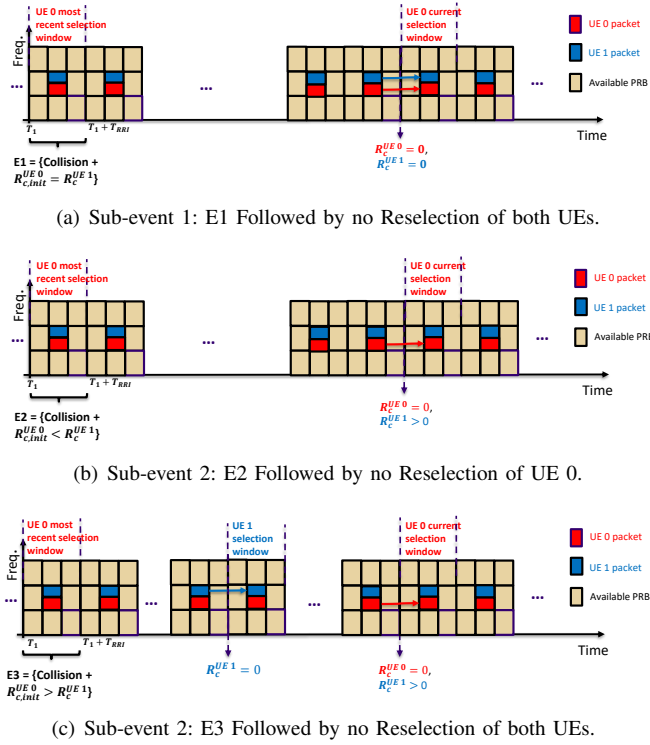


Fig. 10: Events During $[T_1, T_1 + T_{RRI}]$ Followed by UEs' Behaviors that leading Collision Event 2.

reselection (with probability = p_k). The probability that E_2 happens is given by:

$$\Pr\{E_2\} = P_{COL} \cdot \Pr\{R_{c,init}^{UE0} < R_c^{UE1}\} = P_{COL} \cdot \sum_{|I|} \left[\Pr\{R_{c,init}^{UE0} = i\} \cdot \Pr\{R_{c,init}^{UE0} < R_c^{UE1} | R_{c,init}^{UE0} = i\} \right], \quad (15)$$

where $i \in I = \{5, 6, \dots, 15\}$ which is the set of all $R_{c,init}$ states, and $\Pr\{R_{c,init}^{UE0} < R_c^{UE1}\}$ can be obtained according to Fig. 7. Then, the probability that Collision Event 2 happens due to E_2 is thereby derived as

$$P_{COL,2}^{E2} = \Pr\{\text{Collision}|E_2\} \cdot \Pr\{E_2\}, \quad (16)$$

where $\Pr\{\text{Collision}|E_2\} = p_k$.

- $E_3 = \left\{ \text{Collision during } [T_1, T_1 + T_{RRI}], \text{ and } R_{c,init}^{UE0} > R_c^{UE1} \text{ at } T = T_1 + T_{RRI} \right\}$, shown in Fig. 10(c). Then $R_c^{UE1} = 0$ and UE 1 does not perform reselection⁷ (with probability = p_k) before UE 0's current selection window. Afterward, $R_c^{UE0} = 0$ while $R_c^{UE1} > 0$ at the beginning of UE 0's current selection window, and the collision will continue if UE 0 does not perform reselection (with probability = p_k). Then the probability that E_3 happens is given by:

$$\Pr\{E_3\} = P_{COL} \cdot \Pr\{R_{c,init}^{UE0} > R_c^{UE1}\} = P_{COL} \cdot \sum_{|I|} \left[\Pr\{R_{c,init}^{UE0} = i\} \cdot \Pr\{R_{c,init}^{UE0} > R_c^{UE1} | R_{c,init}^{UE0} = i\} \right], \quad (17)$$

⁷We ignore the second-order events and always assume that $R_{c,init}^{UE1} > R_c^{UE0}$ at the end of UE 1's selection window.

where $i \in I = \{5, 6, \dots, 15\}$, and $\Pr\{R_{c,init}^{UE0} > R_c^{UE1}\}$ can be obtained according to Fig. 7. The probability that Collision Event 2 happens due to E_3 is thereby derived as

$$P_{COL,2}^{E3} = \Pr\{\text{Collision}|E_3\} \cdot \Pr\{E_3\}, \quad (18)$$

where $\Pr\{\text{Collision}|E_3\} = p_k^2$.

As $P_{COL,2}^{E1}$, $P_{COL,2}^{E2}$ and $P_{COL,2}^{E3}$ are mutually exclusive, $P_{COL,2}$ can be thereby finalized as:

$$P_{COL,2} = P_{COL,2}^{E1} + P_{COL,2}^{E2} + P_{COL,2}^{E3}. \quad (19)$$

D. Performance Analysis - Packet Reception

The closed-form of MAC collision probability P_{COL} , is obtained by substituting Eq. (12) and (19) into (2), where P_{COL} can be numerically calculated by solving Eq. (8) and (20) simultaneously.

$$P_{COL} = \frac{(1-p_k) \left(1 - \left(1 - \frac{2\pi_0(1-p_k)}{N_a} \right)^{N_{UE}} \right)}{1 - \left(2\pi_0 p_k^2 + p_k \Pr\{R_{c,init}^{UE0} < R_c^{UE1}\} + p_k^2 \Pr\{R_{c,init}^{UE0} > R_c^{UE1}\} \right)}, \quad (20)$$

where the calculation of $\Pr\{R_{c,init}^{UE0} < R_c^{UE1}\}$ and $\Pr\{R_{c,init}^{UE0} > R_c^{UE1}\}$ are shown in Appendix A and B, respectively. We further derive PRR - the probability that a packet is received successfully - which is determined by

- *MAC collision errors*, i.e., Two (or more) UEs transmit packets in the same PRB, and all receive UEs fail to decode those packets; this occurs with probability P_{COL} ;
- *Half-duplex (HD) errors*. These occur because UEs are assumed to be half-duplex devices, incapable of transmitting and receiving simultaneously. Thus, if a transmitter UE and a receiver UE transmit their packets in the same slot, the receiver UE cannot decode the packet from the transmitting UE. The probability that HD errors happen depends on the number of slots in each RRI, given by $P_{HD} = \frac{t_s}{T_{RRI}}$.

If a packet is successfully received, neither MAC collision errors nor HD errors must occur. Thus PRR is given by

$$PRR = (1 - P_{COL})(1 - P_{HD}). \quad (21)$$

IV. MODEL EXTENSION

A. Multiple Layer-2 Packet Transmissions per RRI

To improve the reliability of SL communication, the Packet Data Convergence Protocol (PDCP) duplication mechanism has been standardized in 3GPP [19], whereby a PDCP Packet Data Unit (PDU) is duplicated into two (or more) instances and transmitted on two (or more) PRBs. In this section, we investigate the impact of multiple Layer-2 packet transmissions per RRI.

Since each UE now uses N_{Se} PRBs to transmit N_{Se} identical copies of the PDCP PDU in each RRI, N_{UE} UEs will require $N_{UE}N_{Se}$ PRBs in each RRI as the initial resource pool. Following the logic leading to Eq. (7), the resulting average number of occupied PRBs in the selection window $\bar{N}_o(N_{Se})$, becomes

$$\begin{aligned} \bar{N}_o(N_{Se}) &= N_{UE}N_{Se} - P_{COL}(N_{Se})N_{UE}N_{Se} + \frac{P_{COL}(N_{Se})N_{UE}N_{Se}}{\bar{N}_c(N_{Se})}. \end{aligned} \quad (22)$$

Then the average number of available (unoccupied) PRBs in the selection window, $\overline{N}_a(N_{Se})$, is given by

$$\begin{aligned}\overline{N}_a(N_{Se}) &= N_r - \overline{N}_o(N_{Se}) \\ &= N_r - N_{UE}N_{Se} + \frac{(\overline{N}_c(N_{Se}) - 1)P_{COL}(N_{Se})N_{UE}N_{Se}}{\overline{N}_c(N_{Se})}.\end{aligned}\quad (23)$$

In Collision Event 1, the probability that n -fold collision happens (i.e., at least one of nN_{Se} packets occupy the same PRB as UE 0) given that n UEs participate in reselection is

$$P_r(n, N_{Se}) = 1 - \left(1 - \frac{1}{\overline{N}_a(N_{Se})}\right)^{nN_{Se}}. \quad (26)$$

Substitute Eq. (5) and (26) into (10), yielding:

$$\begin{aligned}\Pr\{\text{Collision}|\text{UE 0 } R_c = 0, \text{ Reselection}\} \\ = 1 - \left(1 + 2\pi_0(1 - p_k) \left(\left(1 - \frac{1}{\overline{N}_a}\right)^{N_{Se}} - 1\right)\right)^{N_{UE}}.\end{aligned}\quad (27)$$

From Eq. (2) and (27), $P_{COL,1}$ in terms of N_{Se} is expressed as

$$P_{COL,1}(N_{Se}) = (1 - p_k) \left[1 - \left(1 + 2\pi_0(1 - p_k) \left(\left(1 - \frac{1}{\overline{N}_a(N_{Se})}\right)^{N_{Se}} - 1\right)\right)^{N_{UE}}\right], \quad (28)$$

where $\overline{N}_a(N_{Se})$ is expressed in Eq. (23). Accordingly, $P_{COL,2}$ expressed in Eq. (19) is modified as follows

$$P_{COL,2}(N_{Se}) = P_{COL}(N_{Se}) \left\{2\pi_0 p_k^2 + p_k \Pr\{R_{c,init}^{UE0} < R_c^{UE1}\} + p_k^2 \Pr\{R_{c,init}^{UE0} > R_c^{UE1}\}\right\}. \quad (29)$$

Then, the closed form of $P_{COL}(N_{Se})$ can be obtained by substituting Eq. (28) and (29) into Eq. (2):

$$P_{COL}(N_{Se}) = \frac{(1 - p_k) \left[1 - \left(1 + 2\pi_0(1 - p_k) \left(\left(1 - \frac{1}{\overline{N}_a(N_{Se})}\right)^{N_{Se}} - 1\right)\right)^{N_{UE}}\right]}{1 - \left(2\pi_0 p_k^2 + p_k \Pr\{R_{c,init}^{UE0} < R_c^{UE1}\} + p_k^2 \Pr\{R_{c,init}^{UE0} > R_c^{UE1}\}\right)}. \quad (30)$$

When $N_{Se} > 1$, a packet transmission is successful if at least one of N_{Se} duplicate packets is correctly decoded. Thus PRR in terms of N_{Se} is given by

$$PRR(N_{Se}) = 1 - \left[1 - \left(1 - P_{COL}(N_{Se})\right)(1 - P_{HD})\right]^{N_{Se}}. \quad (31)$$

where for $N_{Se} = 1$, $P_{COL}(1)$ in Eq. (30) and $PRR(1)$ in Eq. (31) defaults to P_{COL} in Eq. (20) and PRR in Eq. (21), as expected.

B. Proportion of available PRBs for reselection

Another option that possibly improves the SL communication reliability is increasing the minimum proportion of available PRBs for reselection characterized by the parameter X , whose range has been standardized in 3GPP [20], [21]. In the previous sections, the proportion of available (unoccupied) PRBs for reselection was fixed at the lower limit, $X = 0.2$. In this section, we investigate the impact of (higher) X on $P_{COL}(X, N_{Se})$. We show that $P_{COL}(X, N_{Se})$ does not benefit from increasing X , although the number of available PRBs for reselection increases.

In the selection window, the number of available PRBs used for reselection must be first greater than a threshold (i.e., XN_r), which is the required minimum number of PRBs. UE randomly reselects among available PRBs for packet transmissions. In the previous sections, since X is set to a small value (e.g., $X = 0.2$), $\overline{N}_a(N_{Se})$, that represents the number of unoccupied PRBs (referred to as the available PRBs in the previous sections), satisfies $\overline{N}_a(N_{Se}) > XN_r$ in the under-saturated condition. However, $\overline{N}_a(N_{Se}) > XN_r$ may not hold if X is increased significantly: UE has to increase $\overline{N}_a(N_{Se})$ to XN_r by including $XN_r - \overline{N}_a(N_{Se})$ occupied PRBs in order to satisfy the minimum number requirement of total XN_r available PRBs for reselection. Thus, the XN_r available PRBs now include $\overline{N}_a(N_{Se})$ unoccupied PRBs and $XN_r - \overline{N}_a(N_{Se})$ occupied PRBs. In Collision Event 1, if $\overline{N}_a(N_{Se}) < XN_r$, two collision cases happen given that UE 0 performs reselection in the selection window:

- *Case 1:* UE 0 selects one of the $\overline{N}_a(N_{Se})$ unoccupied PRBs among XN_r available PRBs, and a collision happens if another UE reselects the same unoccupied PRB as UE 0;
- *Case 2:* Collision happens if UE 0 selects one of the $XN_r - \overline{N}_a(N_{Se})$ occupied PRBs among XN_r available PRBs.

Regarding Case 1, the probability that UE 0 selects one of the unoccupied PRBs among XN_r available PRBs is $\frac{\overline{N}_a(N_{Se})}{XN_r}$. Meanwhile, the probability that collision happens is expressed in Eq. (27); Regarding Case 2, the probability that UE 0 selects one of the occupied PRBs among XN_r PRBs is $\frac{XN_r - \overline{N}_a(N_{Se})}{XN_r}$, and the probability that collision happens is 1. Thus $P_{COL,1}(X, N_{Se})$ under $\overline{N}_a(N_{Se}) < XN_r$ is given by Eq. (24), where $\overline{N}_a(N_{Se})$ (that denotes the number of unoccupied PRBs in the selection window) is expressed in Eq. (23). Then, the closed form of $P_{COL}(N_{Se}, X)$ under $\overline{N}_a(N_{Se}) < XN_r$ can be obtained by substituting Eq. (24) and (29) into Eq. (2); meanwhile, $P_{COL}(N_{Se}, X) = P_{COL}(N_{Se})$ under $\overline{N}_a(N_{Se}) \geq XN_r$, where $P_{COL}(N_{Se})$ is given by Eq. (30). As a result, $P_{COL}(N_{Se}, X)$ is expressed in Eq. (25), where $\overline{N}_a(N_{Se})$ is expressed in Eq. (23). Accordingly, the PRR in terms of X is given by

$$PRR(N_{Se}, X) = 1 - \left[1 - \left(1 - P_{COL}(N_{Se}, X)\right)(1 - P_{HD})\right]^{N_{Se}}. \quad (32)$$

Meanwhile, the average number of available PRBs in the selection window, $\overline{N}_a(N_{Se}, X)$, is given by

$$\overline{N}_a(N_{Se}, X) = \begin{cases} \overline{N}_a(N_{Se}) & \text{for } \overline{N}_a(N_{Se}) \geq XN_r, \\ XN_r & \text{for } \overline{N}_a(N_{Se}) < XN_r, \end{cases} \quad (33)$$

where $\overline{N}_a(N_{Se})$ is given by Eq. (23).

$$P_{COL,1}(N_{Se}, X) = (1 - p_k) \left\{ \left[1 - \left(1 + 2\pi_0(1 - p_k) \left(\left(1 - \frac{1}{\bar{N}_a(N_{Se})} \right)^{N_{Se}} - 1 \right) \right)^{N_{UE}} \right] \cdot \frac{\bar{N}_a(N_{Se})}{X N_r} + 1 \cdot \frac{X N_r - \bar{N}_a(N_{Se})}{X N_r} \right\}, \quad (24)$$

$$P_{COL}(N_{Se}, X) = \begin{cases} P_{COL}(N_{Se}) & \text{for } \bar{N}_a(N_{Se}) \geq X N_r, \\ \frac{(1 - p_k) \left\{ \left[1 - \left(1 + 2\pi_0(1 - p_k) \left(\left(1 - \frac{1}{\bar{N}_a(N_{Se})} \right)^{N_{Se}} - 1 \right) \right)^{N_{UE}} \right] \cdot \frac{\bar{N}_a(N_{Se})}{X N_r} + 1 \cdot \frac{X N_r - \bar{N}_a(N_{Se})}{X N_r} \right\}}{1 - \left(2\pi_0 p_k^2 + p_k \Pr\{R_{c,init}^{UE0} < R_c^{UE1}\} + p_k^2 \Pr\{R_{c,init}^{UE0} > R_c^{UE1}\} \right)} & \text{for } \bar{N}_a(N_{Se}) < X N_r. \end{cases} \quad (25)$$

V. MODEL VALIDATION

A. Simulation Description

To validate the predicted performance for the asynchronous R_c decrementation based on our model, we resort to simulations using ns-3⁸ by building off the 5G-LENA module as a base [7], [22]⁹. The main parameters used during the ns-3 simulation can be found in Table II.

TABLE II: Main ns-3 Simulation Parameters

Parameter	Value	Parameter	Value
N_{sc}	2	P_t	23 dBm
t_s	1 ms	T_{RRI}	100 ms
γ_{SPS}	-110 dBm	N_{UE}	[20, 200]
p_k	[0, 0.8]	X	[0.2, 0.5]

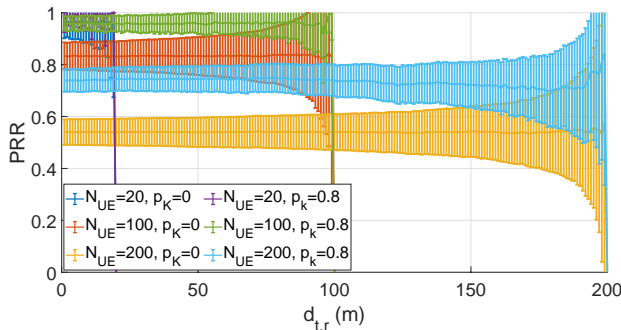


Fig. 11: Simulated $PRR(d_{t,r})$ in the Fully Connected Network.

Simulations were conducted for a linear topology with N_{UE} UEs in a single row separated by 1 meter, allowing them to transmit periodic safety messages according to the V2X mode 2 algorithm. Each simulation took place over the course of 100 seconds, the first 40 of which were excised to eliminate initialization effects for a total of 60 seconds of data. Each parameter set was repeated once with a new seed to ensure sufficient samples were taken to report data with high confidence. The only source of randomness in the simulation is the choice of PRB; thus a single, long simulation is sufficient to capture that randomness. ns-3 simulation runs produce traces of Physical Sidelink Control Channel (PSCCH) and Physical Sidelink

Shared Channel (PSSCH) transmissions and receptions by all UEs (over slot and sub-channel used), that are post-processed to derive simulation estimates of P_{COL} and associated sub-events. This is achieved by observing instances of UEs using identical PRBs and tracing the channel's history to determine the type of collision. N_C is determined simultaneously as P_{COL} by counting the number of PSCCH/PSSCH transmissions in the PRB during collisions. The PRR is derived by counting the number of successfully decoded PSSCH¹⁰ transmissions. In the case of $N_{Se} > 1$, more than one successful duplicate PSSCH decode counts as one for the PRR calculation. N_a is derived from a separate trace from the SPS algorithm, which measures N_a directly during each reselection event for each UE. In addition to the previously mentioned metrics, we tested the PRR as a function of distance up to the largest N_{UE} tested (200 UEs result in 200 meters) to ensure the network was fully connected. Fig. 11 proves that PRR is uniform over all possible distances; thus, there is no dependence on distance. The ns-3 simulation was conducted on a PC running Ubuntu 20.04 with AMD Ryzen 9 3900X 12-Core Processor 3.79 GHz while the data processing and analytical models were implemented using Matlab R2023b.

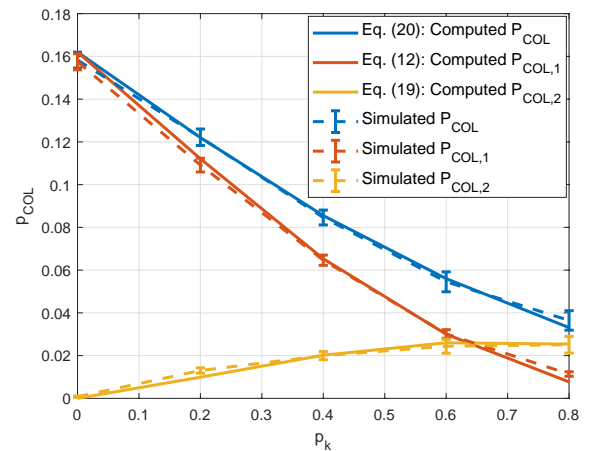


Fig. 12: P_{COL} in terms of p_k : $N_{UE} = 100$.

⁸Open source network simulator, available @ www.nsnam.org.

⁹All code used to generate both modeled and simulated curves can be found at <https://github.com/CollinBrady1993/Code-for-NR-C-V2X-Tutorial>.

¹⁰In ns-3, a successful PSSCH decode requires the corresponding PSCCH to be decoded as well.

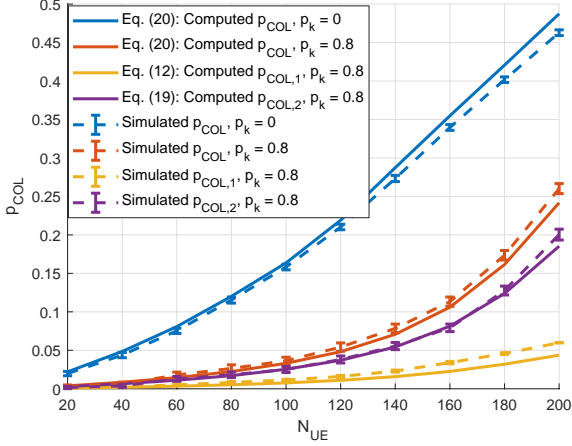


Fig. 13: P_{COL} in terms of N_{UE} : $p_k = 0/0.8$.

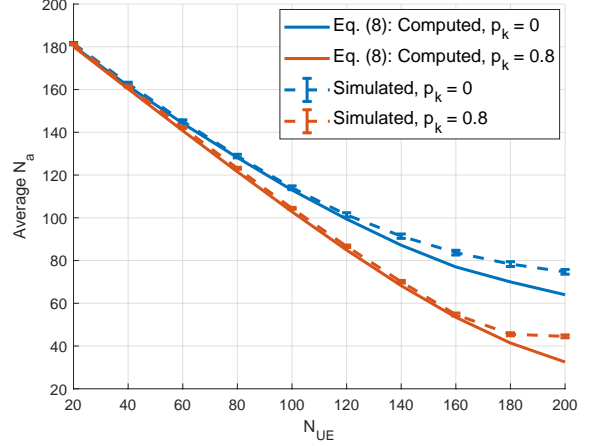


Fig. 14: \overline{N}_a in terms of N_{UE} : $p_k = 0/0.8$.

B. Validation Results

P_{COL} vs p_k , fixed N_{UE} (Fig. 12): We observe that both P_{COL} and $P_{COL,1}$ monotonically decreases with p_k while $P_{COL,2}$ is monotonic increasing. The decrease of $P_{COL,1}$ can be explained by Eq. (12): when p_k increases, UE 0 performs reselection less frequently in the selection window; meanwhile, the term $1 - \left(1 - \frac{2\pi_0(1-p_k)}{\overline{N}_a}\right)^{N_{UE}}$ also decreases, indicating that UE 0 is less likely to collide with other UEs given that UE 0 performs reselection in the selection window. Both effects cause $P_{COL,1}$ to decrease. The increase of $P_{COL,2}$ with p_k can be explained as follows: when p_k increases, UE 0 does not reselect more frequently in the selection window; meanwhile, if UE 0 collides with another UE in the selection window, their consecutive collisions last longer because they are more likely to stick with the previously reserved PRB. Since the decrease of $P_{COL,1}$ is much more significant than the increase of $P_{COL,2}$, P_{COL} thereby increases with p_k . Note that the cross-over point between $P_{COL,1}$ and $P_{COL,2}$ occurs at $p_k \approx 0.64$, it follows that Collision Event 1 happens more frequently than Collision Event 2 in most p_k cases (i.e., $p_k \in [0, 0.64]$). We conclude by remarking that the proposed models for P_{COL} , $P_{COL,1}$ and $P_{COL,2}$ matches well the ns-3 simulation results for a typical scenario ($N_{UE} = 100$).

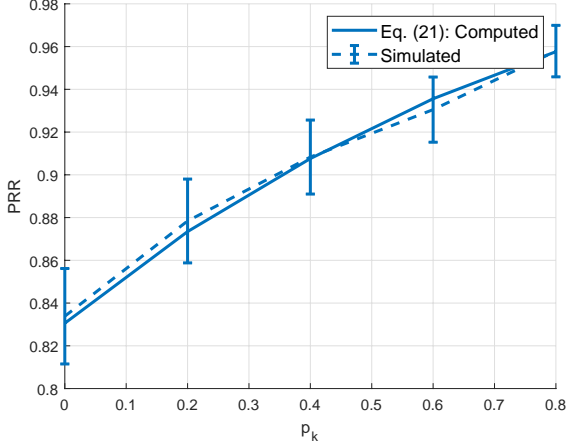
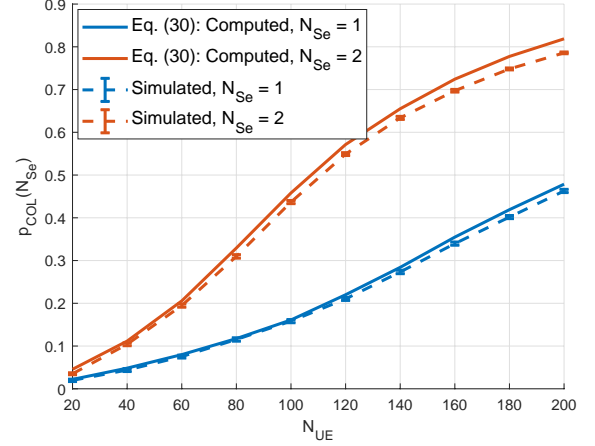
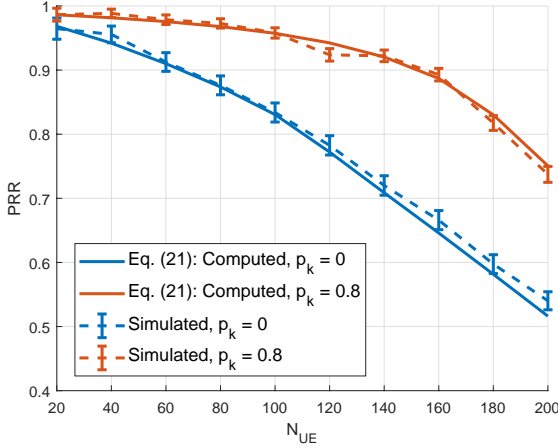
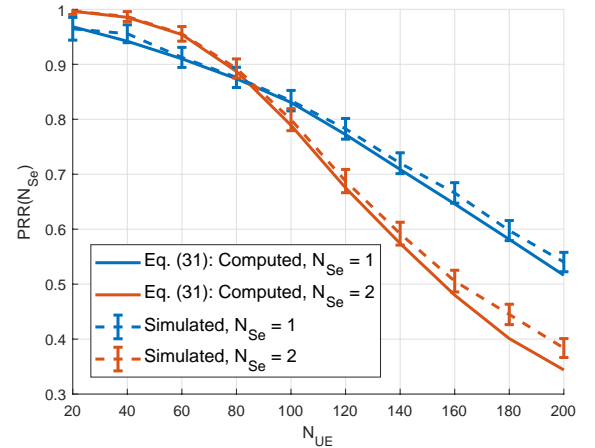
P_{COL} vs N_{UE} , varied p_k (Fig. 13): Next, the computed P_{COL} , $P_{COL,1}$ and $P_{COL,2}$ overall matches the simulated ones at different N_{UE} . Note that when $p_k = 0$, only Collision Event 1 happens, thus $P_{COL} = P_{COL,1}$. When N_{UE} goes up, both P_{COL} under two p_k go up. For $p_k = 0$, with increasing N_{UE} , more UEs participate in reselection, which leads P_{COL} to increase. Hence for $p_k = 0.8$ and higher N_{UE} , likelihood of Collision Event 2 (which dominates P_{COL}) is higher, which leads P_{COL} to increase. Compared with the simulation results, the analytical model subtly overestimates P_{COL} with $p_k = 0$ at $N_{UE} \geq 160$. This gap can be explained by the \overline{N}_a difference shown in Fig. 14. The computed \overline{N}_a is very close to the simulated values at low N_{UE} , however, the computed \overline{N}_a deviates from the simulated one around $N_{UE} \geq 160$. The lower \overline{N}_a indicates that

each UE has fewer available PRBs for reselection, and two UEs are more likely to re-select the same available PRB. Therefore, the computed P_{COL} is overestimated compared to the simulated P_{COL} at high N_{UE} . Note that the total number of PRBs in each RRI is $N_r = 200$ while the channel moves to saturation for $N_{UE} \geq 160$. Thus, the proposed analytical model can accurately predict P_{COL} and \overline{N}_a in an under-saturated condition while it becomes less accurate in a saturated condition ($N_{UE} \approx N_r$). This is due to PHY issues that must be incorporated into the analysis for better accuracy under the saturated condition. For instance, large numbers of UEs in a dense local network imply that their respective RSRPs at a receiver are closer in value. As a result, when the RSRP threshold is increased to include more available PRBs for reselection, the actual \overline{N}_a might be higher than the computed \overline{N}_a in a saturated condition, rendering the pure MAC analysis less accurate. Note that saturated channel assumption is impractical for SL communications operationally, because the significant PRR decrease will not satisfy the desired Quality of Service (QoS) requirements for critical BSMs or status messages.

PRR vs p_k , fixed N_{UE} (Fig. 15): At $N_{UE} = 100$ (an under-saturated case), the computed PRR matches quite well with the simulated one under different p_k , and PRR increases as p_k increases. PRR vs N_{UE} , varied p_k (Fig. 16): Meanwhile, the computed PRR also matches with the simulated one at different N_{UE} . Note that the computed PRR with $p_k = 0$ at high N_{UE} is subtly lower than the simulated one because the computed P_{COL} with $p_k = 0$ is overestimated at high N_{UE} .

$P_{COL}(N_{Se})$ vs N_{UE} , fixed p_k (Fig. 17): The computed $P_{COL}(N_{Se})$ overall matches with the simulated $P_{COL}(N_{Se})$ at different N_{UE} , especially in the under-saturated condition. As expected, for a given P_{COL} (e.g., $P_{COL} = 0.1$), $N_{UE} \approx 80$ for $N_{Se} = 1$ is almost twice of $N_{UE} \approx 40$ for $N_{Se} = 2$. Meanwhile, at the lower N_{UE} (e.g., $N_{UE} = 60$), $P_{COL}(2)$ (≈ 0.2) is almost twice of $P_{COL}(1)$ (≈ 0.1). Also, it is clear that $P_{COL}(2)$ is always higher than $P_{COL}(1)$ for all N_{UE} .

$PRR(N_{Se})$ vs N_{UE} , fixed p_k (Fig. 18): However, the

Fig. 15: PRR in terms of p_k : $N_{UE} = 100$.Fig. 17: $P_{COL}(N_{Se})$ in terms of N_{UE} : $p_k = 0$.Fig. 16: PRR in terms of N_{UE} : $p_k = 0/0.8$.Fig. 18: $PRR(N_{Se})$ in terms of N_{UE} : $p_k = 0$.

$PRR(N_{Se})$ does not always follow the behavior of $P_{COL}(N_{Se})$ vs N_{UE} . For under-saturated condition, e.g., $N_{UE} \leq 80$, $PRR(2)$ is always higher than $PRR(1)$. Note that per Eq. (31), $PRR(N_{Se})$ is proportional to $1 - (P_{COL}(N_{Se}))^{N_{Se}}$ if P_{HD} is neglected (N_{Se} does not affect P_{HD}), where $(P_{COL}(N_{Se}))^{N_{Se}}$ represents the probability that all N_{Se} packets are not decoded. In the under-saturated condition, $N_{Se} = 2$ improves the packet reception gain because $P_{COL}(1) > (P_{COL}(2))^2$. However, when $N_{UE} \geq 100$ (saturated scenario), $PRR(2)$ significantly dominates $PRR(1)$. Thus $PRR(N_{Se} = 2)$ degrades significantly due to $P_{COL}(1) < (P_{COL}(2))^2$. Note that the cross-over value $(N_{UE}^*, PRR(N_{Se}, N_{UE}^*))$ represents the performance boundary in terms of N_{UE} and N_{Se} : $PRR(N_{Se}, N_{UE})$ benefits from the larger N_{Se} if $N_{UE} < N_{UE}^*$, and degrades if $N_{UE} > N_{UE}^*$. N_{UE}^* can be determined by solving $PRR(1, N_{UE}^*) = PRR(2, N_{UE}^*)$.

$\bar{N}_a(N_{Se})$ vs N_{UE} , fixed p_k (Fig. 19): The computed $\bar{N}_a(1)$ is close to the simulated value when $N_{UE} < 160$ while $\bar{N}_a(2)$ matches with the simulated when $N_{UE} < 100$ representing the

under-saturated condition ($N_{UE} \leq 160$ for $N_{Se} = 1$ and $N_{UE} \leq 100$ for $N_{Se} = 2$). Thus, computed $\bar{N}_a(N_{Se})$ is accurately in the under-saturated condition. In addition, the $\bar{N}_a(N_{Se})$ difference for $N_{Se} = 2$ becomes quite large in the saturated condition. For instance, when $N_{UE} = 200$ and $N_{Se} = 2$, the number of packets transmitted in each RRI is $N_{UE}N_{Se} = 400$, which is twice the total number of PRBs in each RRI $N_r = 200$. It should be noted that the simulated $\bar{N}_a(N_{Se})$ goes up as N_{UE} increases in the saturated condition. This behavior occurs because the measured RSRP of each PRB becomes very close in the saturated condition, and some of the available PRBs for reselection become occupied. Increasing the RSRP threshold (e.g., 3dB granularity is increased each time) will include a burst of PRBs: the more the packets are transmitted in the saturated condition, the more the PRBs are included within each 3 dB granularity, and the higher the $\bar{N}_a(N_{Se})$ in the simulation is, which contradicts the fact in the model that more transmitted packets lead to the lower $\bar{N}_a(N_{Se})$. Thus, the pure MAC analysis becomes less accurate regarding $P_{COL}(N_{Se})$ and $PRR(N_{Se})$ in the saturated condition.

$P_{COL}(1, X)$ and $PRR(1, X)$ vs N_{UE} , fixed p_k (Fig. 20 and

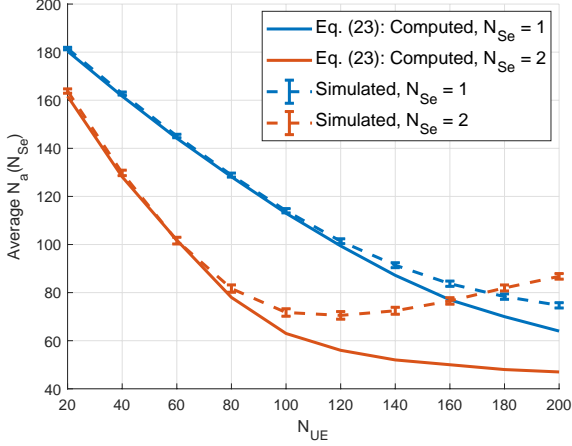


Fig. 19: $\overline{N}_a(N_{Se})$ in terms of N_{UE} : $p_k = 0$.

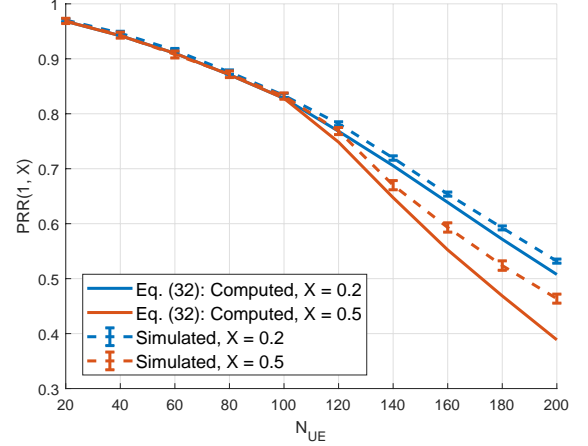


Fig. 21: $PRR(1, X)$ in terms of N_{UE} : $p_k = 0$.

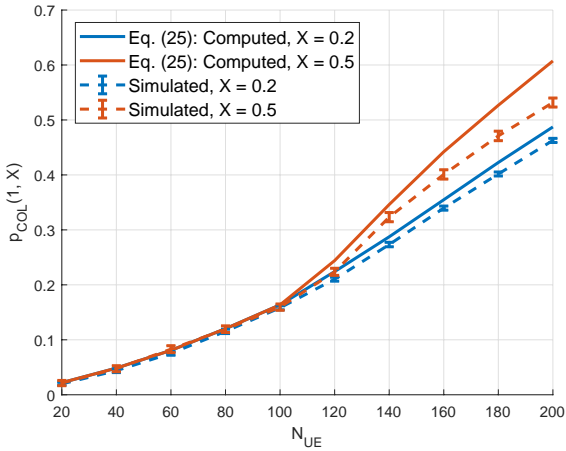


Fig. 20: $P_{COL}(1, X)$ in terms of N_{UE} : $p_k = 0$.

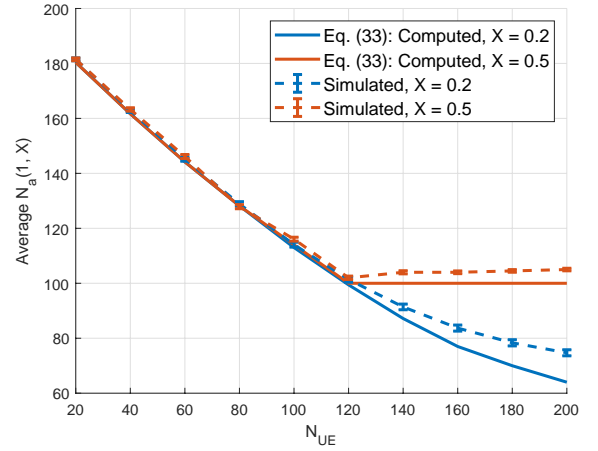


Fig. 22: $\overline{N}_a(1, X)$ in terms of N_{UE} : $p_k = 0$.

21): The computed $P_{COL}(1, X)$ and $PRR(1, X)$ are validated to predict well based on the simulated ones in the under-saturated channel condition. Meanwhile, $\overline{N}_a(1, X)$ in terms of N_{UE} is validated in Fig. 22. Note that, according to Eq. (33), the minimum $\overline{N}_a(1, 0.2) = 0.2 \cdot 200 = 40$ while the minimum $\overline{N}_a(1, 0.5) = 0.5 \cdot 200 = 100$. $\overline{N}_a(1)$ in both cases (only including unoccupied PRBs in available PRBs) must be the same if $\overline{N}_a(1) \geq 100$. Therefore, when $N_{UE} \leq 100$, indicating that $\overline{N}_a(1) \geq 100$, $P_{COL}(1, 0.5)$ (or $PRR(1, 0.5)$) should be the same as $P_{COL}(1, 0.2)$ (or $PRR(1, 0.2)$), which is validated in Fig. 20 (or Fig. 21). As N_{UE} further increases, meaning that $\overline{N}_a(1) < 100$, $\overline{N}_a(1, 0.5) = 100$ (including both unoccupied and occupied PRBs in available PRBs) remains fixed. By contrast, $\overline{N}_a(1, 0.2)$ keeps decreasing because $\overline{N}_a(1) > 40$ still holds (only including unoccupied PRBs in available PRBs). As a result, $P_{COL}(1, 0.5)$ (or $PRR(1, 0.5)$) is no longer the same as $P_{COL}(1, 0.2)$ (or $PRR(1, 0.2)$) in such cases.

VI. CONCLUSION

In this work, we developed novel MAC collision models to thoroughly investigate the performance of the SPS protocol for 5G NR SL. Particularly, we defined the MAC collision events that accurately characterized the essence of MAC-based SPS. We also showed how the key SPS features relate to and further determine the MAC collision performance. The computed results were validated via simulations using the 5G-LENA module in ns-3. Through the extended analytical models, we illustrated that the MAC PRR benefits from the new feature - multiple Layer-2 packet transmission (N_{Se}) only in the under-saturated channel condition. Meanwhile, setting another feature - the minimum proportion of available PRBs for reselection (X) greater than 0.2 for the safety-related messages provides no benefit in any channel condition. Hence, we recommend that network engineers always set X to the minimum allowable value and 3GPP consider lowering the current lower limit of $X = 0.2$ for SL reliability enhancement.

As the proposed pure MAC-based model does not work well in the saturated channel condition due to PHY issues, future

work will adapt the current model by incorporating relevant PHY parameters to address the above problem. In addition, it would be interesting to validate if the proposed NR mode 2 MAC PRR model is also compatible with the LTE mode 4 under the same SPS configurations.

APPENDIX

A. $\Pr\{R_{c,init}^{UE0} < R_c^{UE1}\}$ calculation

According to Fig. 7 and Eq. (15),

$$\begin{aligned}
& \Pr\{R_{c,init}^{UE0} < R_c^{UE1}\} \\
&= \sum_{|I|} \Pr\{R_{c,init}^{UE0} = i\} \cdot \Pr\{R_{c,init}^{UE0} < R_c^{UE1} | R_{c,init}^{UE0} = i\} \\
&= \Pr\{R_c^{UE1} = 0 | R_c^{UE0} = 0 \text{ during UE 0 most recent selection window}\} \\
&\quad \cdot \Pr\{R_{c,init}^{UE1} > R_{c,init}^{UE0} \text{ during UE 0 most recent selection window}\} + \\
&\Pr\{R_c^{UE1} \neq 0 | R_c^{UE0} = 0 \text{ during UE 0 most recent selection window}\} \\
&\quad \cdot \Pr\{R_{c,init}^{UE1} > R_{c,init}^{UE0} \text{ during UE 0 most recent selection window}\} \\
&= 2\pi_0 \frac{5}{11} + (1 - 2\pi_0) \left(\frac{1}{11} \cdot \frac{5}{11} + \frac{1}{11} \cdot \frac{45}{121} + \frac{1}{11} \cdot \frac{36}{121} \frac{1}{11} \cdot \frac{28}{121} + \right. \\
&\quad \left. \frac{1}{11} \cdot \frac{21}{121} + \frac{1}{11} \cdot \frac{15}{121} + \frac{1}{11} \cdot \frac{10}{121} \frac{1}{11} \cdot \frac{6}{121} + \frac{1}{11} \cdot \frac{3}{121} + \frac{1}{11} \cdot \frac{1}{121} + \right. \\
&\quad \left. \frac{1}{11} \cdot \frac{0}{121} \right) \\
&= 0.2892 \cdot 2\pi_0 + 0.1653.
\end{aligned} \tag{34}$$

B. $\Pr\{R_{c,init}^{UE0} > R_c^{UE1}\}$ calculation

According to Fig. 7 and Eq. (17),

$$\begin{aligned}
& \Pr\{R_{c,init}^{UE0} > R_c^{UE1}\} \\
&= \sum_{|I|} \Pr\{R_{c,init}^{UE0} = i\} \cdot \Pr\{R_{c,init}^{UE0} > R_c^{UE1} | R_{c,init}^{UE0} = i\} \\
&= \Pr\{R_c^{UE1} = 0 | R_c^{UE0} = 0 \text{ during UE 0's most recent selection window}\} \\
&\quad \cdot \Pr\{R_{c,init}^{UE1} < R_{c,init}^{UE0} \text{ during UE 0's most recent selection window}\} + \\
&\Pr\{R_c^{UE1} \neq 0 | R_c^{UE0} = 0 \text{ during UE 0's most recent selection window}\} \\
&\quad \cdot \Pr\{R_{c,init}^{UE1} < R_{c,init}^{UE0} \text{ during UE 0's most recent selection window}\} \\
&= 2\pi_0 \frac{5}{11} + (1 - 2\pi_0) \left(\frac{1}{11} \cdot \frac{5}{11} + \frac{1}{11} \cdot \frac{6}{11} + \frac{1}{11} \cdot \frac{76}{121} + \frac{1}{11} \cdot \frac{85}{121} + \right. \\
&\quad \left. \frac{1}{11} \cdot \frac{93}{121} + \frac{1}{11} \cdot \frac{100}{121} + \frac{1}{11} \cdot \frac{106}{121} + \frac{1}{11} \cdot \frac{111}{121} + \frac{1}{11} \cdot \frac{115}{121} + \frac{1}{11} \cdot \frac{118}{121} + \right. \\
&\quad \left. \frac{1}{11} \cdot \frac{120}{121} \right) \\
&= 0.7851 - 0.3306 \cdot 2\pi_0.
\end{aligned} \tag{35}$$

REFERENCES

- [1] V. Weerackody, K. Benson, and S. Roy, "Who Needs Basestations When We Have Sidelinks?" *Global Communications*, vol. 2023, 2023.
- [2] FirstNet, "First Responder Network Authority," www.firstnet.gov.
- [3] 3GPP, "Study on NR Vehicle-to-Everything (V2X)," The 3rd Generation Partnership Project (3GPP), Tech. Rep. TR37.885, Mar 2019.
- [4] A. Nabil, K. Kaur, C. Dietrich, and V. Marojevic, "Performance analysis of sensing-based semi-persistent scheduling in C-V2X networks," in *2018 IEEE 88th vehicular technology conference (VTC-Fall)*. IEEE, 2018, pp. 1–5.
- [5] G. Cecchini, A. Bazzi, B. M. Masini, and A. Zanella, "LTEV2Vsim: An LTE-V2V simulator for the investigation of resource allocation for cooperative awareness," in *2017 5th IEEE International Conference on Models and Technologies for Intelligent Transportation Systems (MT-ITS)*. IEEE, 2017, pp. 80–85.
- [6] B. McCarthy and A. O'Driscoll, "OpenCV2X mode 4: A simulation extension for cellular vehicular communication networks," in *2019 IEEE 24th International Workshop on Computer Aided Modeling and Design of Communication Links and Networks (CAMAD)*. IEEE, 2019, pp. 1–6.
- [7] Z. Ali, S. Lagén, L. Giupponi, and R. Rouil, "3GPP NR V2X mode 2: overview, models and system-level evaluation," *IEEE Access*, vol. 9, pp. 89 554–89 579, 2021.
- [8] C. Campolo, A. Molinaro, F. Romeo, A. Bazzi, and A. O. Berthet, "5G NR V2X: On the impact of a flexible numerology on the autonomous sidelink mode," in *2019 IEEE 2nd 5G World Forum (5GWF)*. IEEE, 2019, pp. 102–107.
- [9] A. Bazzi, G. Cecchini, A. Zanella, and B. M. Masini, "Study of the impact of PHY and MAC parameters in 3GPP C-V2V mode 4," *IEEE Access*, vol. 6, pp. 71 685–71 698, 2018.
- [10] M. Chen, R. Chai, H. Hu, W. Jiang, and L. He, "Performance evaluation of C-V2X mode 4 communications," in *2021 IEEE Wireless Communications and Networking Conference (WCNC)*. IEEE, 2021, pp. 1–6.
- [11] P. Liu, C. Shen, C. Liu, F. J. Cintrón, L. Zhang, L. Cao, R. Rouil, and S. Roy, "Towards 5G new radio sidelink communications: A versatile link-level simulator and performance evaluation," *Computer Communications*, 2023.
- [12] A. Rehman, P. Di Marco, R. Valentini, and F. Santucci, "Analytical modeling of multiple access interference in C-V2X sidelink communications," in *2022 IEEE International Mediterranean Conference on Communications and Networking (MeditCom)*. IEEE, 2022, pp. 215–220.
- [13] A. Rehman, R. Valentini, E. Cinque, P. Di Marco, and F. Santucci, "On the impact of multiple access interference in LTE-V2X and NR-V2X sidelink communications," *Sensors*, vol. 23, no. 10, p. 4901, 2023.
- [14] M. Gonzalez-Martín, M. Sepulcre, R. Molina-Masegosa, and J. Gozalvez, "Analytical models of the performance of C-V2X mode 4 vehicular communications," *IEEE Transactions on Vehicular Technology*, vol. 68, no. 2, pp. 1155–1166, 2018.
- [15] X. Gu, J. Peng, Y. Cheng, X. Zhang, W. Liu, Z. Huang, and L. Cai, "Performance analysis on access collision in semi-persistent scheduling of C-V2X mode 4," in *2021 IEEE 94th Vehicular Technology Conference (VTC2021-Fall)*. IEEE, 2021, pp. 1–5.
- [16] X. Gu, J. Peng, L. Cai, Y. Cheng, X. Zhang, W. Liu, and Z. Huang, "Performance Analysis and Optimization for Semi-Persistent Scheduling in C-V2X," *IEEE Transactions on Vehicular Technology*, vol. 72, no. 4, pp. 4628–4642, 2022.
- [17] G. P. W. NBA, J. Haapola, and T. Samarasinghe, "A discrete-time Markov chain based comparison of the MAC layer performance of C-V2X mode 4 and IEEE 802.11 p," *IEEE Transactions on Communications*, vol. 69, no. 4, pp. 2505–2517, 2020.
- [18] M. H. C. Garcia, A. Molina-Galan, M. Boban, J. Gozalvez, B. Coll-Perales, T. Şahin, and A. Kousaridas, "A tutorial on 5G NR V2X communications," *IEEE Communications Surveys & Tutorials*, vol. 23, no. 3, pp. 1972–2026, 2021.
- [19] 3GPP, "Overall description of radio access network (RAN) aspects for vehicle-to-everything (V2X) based on LTE and NR," The 3rd Generation Partnership Project (3GPP), Tech. Rep. TR37.985, Jul 2020.
- [20] —, "Evolved Universal Terrestrial Radio Access (E-UTRA); Physical layer procedures," The 3rd Generation Partnership Project (3GPP), Tech. Rep. TR36.213, Dec 2020.
- [21] —, "Evolved universal terrestrial radio access (E-UTRA); medium access control (MAC) protocol specification," The 3rd Generation Partnership Project (3GPP), Tech. Rep. TR36.321, Dec 2020.
- [22] C. Brady, L. Cao, and S. Roy, "Modeling of NR C-V2X Mode 2 Throughput," in *2022 IEEE International Workshop Technical Committee on Communications Quality and Reliability (CQR)*. IEEE, 2022, pp. 19–24.